# Project 048 Analysis to Support the Development of an Engine nvPM Emissions Standard

## Massachusetts Institute of Technology

## Project Lead Investigator

Steven Barrett
Associate Professor
Department of Aeronautics & Astronautics
Massachusetts Institute of Technology
77 Massachusetts Ave
Building 33-316
Cambridge, MA 02139
617-452-2550
sbarrett@mit.edu

## University Participants

**Massachusetts Institute of Technology**

- PI: Professor Steven Barrett
- Co-PI: Dr. Raymond Speth
- FAA Award Number: 13-C-AJFE-MIT, Amendment Nos. 027, 036, 045, 054, 065, 069, 083, and 087
- Period of Performance: July 8, 2016 to November 30, 2022 (reporting here with the exception of funding level and cost share only for the period October 1, 2020 to September 30, 2021)
- Tasks:
    1. Developing a no-change criterion for engine re-measurement
    2. Extending the non-volatile particulate matter (nvPM) fuel correction method for blended fuels
    3. Analyze emissions data collected for the Committee on Aviation Environmental Protection (CAEP)/10 nvPM standard
    4. Evaluating cruise emissions based on ground-based measurements

## Project Funding Level

The funding included $950,000 FAA funding and $950,000 matching funds. The matching funds comprised approximately $214,000 from MIT, plus third-party in-kind contributions of $87,000 from University College London, $158,000 from Oliver Wyman Group, $156,000 from Byogy Renewables, Inc., $153,000 from NuFuels LLC, and $182,000 from Savion Aerospace Corp.

## Investigation Team

- Professor Steven Barrett (MIT) serves as PI for the A48 project as head of the Laboratory for Aviation and the Environment. Professor Barrett coordinates internal research efforts and maintains communication among investigators in the various MIT research teams.
- Dr. Raymond Speth (MIT) serves as co-PI for the A48 project. Dr. Speth directly advises student research in the Laboratory for Aviation and the Environment focused on assessment of fuel and propulsion system technologies targeting reduction of aviation's environmental impacts. Dr. Speth also coordinates communication with FAA counterparts.
- Dr. Jayant Sabnis (MIT) serves as co-investigator for the A48 project. Dr. Sabnis co-advises student research in the Laboratory for Aviation and the Environment. His research interests include turbomachinery, propulsion systems, gas turbine engines, and propulsion system–airframe integration.

- Akshat Agarwal (MIT) was a graduate student in the Laboratory for Aviation and the Environment. Until graduating in 2021, he was responsible for conducting the cost–benefit analysis of the nvPM emissions standard and developing methods for estimating nvPM emissions based on smoke number measurements.
- Dr. Bang-Shiuh Chen (MIT) is a postdoctoral associate in the Laboratory for Aviation and the Environment. He is primarily responsible for evaluating and improving models for estimating full-flight emissions from certification measurements.

# Project Overview

The FAA's Office of Environment and Energy (FAA-AEE) is working with the international community to implement an international aircraft engine nvPM standard for engines with rated thrust greater than 26.7 kN. The proposed nvPM standard will influence the development of future engine technologies, thus resulting in the reduction of nvPM emissions from aircraft engines, and consequently leading to improved human health and climate impacts of aviation. During the CAEP/11 cycle, the FAA, alongside other national aviation authorities, developed an nvPM emissions standard for the mass and particle number emitted by aircraft engines. During the current cycle (CAEP/12), the FAA requires support to provide a technical basis for the implementation of the nvPM emissions standards.

# Task 1 - Developing a No-change Criterion for Engine Re-measurement

Massachusetts Institute of Technology

## Objective

The objective of this task was to identify when an engine, after small changes are made to it, needs its emissions remeasured.

## Research Approach

The landing and takeoff (LTO) nvPM mass and number standards were developed and agreed upon during CAEP/11. This process identified the total emissions per unit rated thrust that an engine can emit during the LTO procedure as the quantity to be evaluated. For gaseous emissions and the CAEP/10 maximum mass concentration standard, allowances are made for small changes to the engine design, which do not require emissions re-certification. In this task, we developed no-change criteria for the CAEP/11 LTO nvPM mass and number standards, on the basis of the uncertainty of the nvPM mass and number measurement system. If an engine's nvPM mass or number metric value (MV = $D_p/F_{00}$) is estimated to change by more than the combined uncertainty of the underlying measurements, then an engine should be retested because there is statistical certainty that the emissions of the engine have changed.

To quantify the uncertainty of an MV, we first introduce the approach to estimate it. It is calculated as:

$$\mathrm{MV} = \frac{D_p}{F_{00}} = \frac{\sum_{i=1}^{4} \mathrm{EI}_i \dot{m}_{f,i}}{F_{00}}$$

where $D_p$ is the total LTO emissions, $F_{00}$ is the engine rated thrust, $\mathrm{EI}_i$ is the emissions index in International Civil Aviation Organization (ICAO) mode of operation $i$, and $\dot{m}_f$ is the fuel flow rate. To calculate each $\mathrm{EI}_i$, we use:

$$\mathrm{EI}_m\left[\frac{\mathrm{mg}}{\mathrm{kg_f}}\right] = \frac{22.4\times10^{-3}\,\mathrm{nvPM}_m\,k_t k_f}{\left([\mathrm{CO_2}]_{\mathrm{dil}} + \frac{1}{\mathrm{DF_1}}([\mathrm{CO}] - [\mathrm{CO_2}]_{\mathrm{b}} + [\mathrm{HC}])\right)(M_C + \alpha M_H)}$$

where $\mathrm{nvPM}_m$ is the mass concentration, $k_t$ is the thermophoretic correction, $k_f$ is the fuel correction, $[X]$ is the diluted mass concentration of species $X$, $\mathrm{DF_1}$ is dilution factor 1, $M_C = 12.0$ g/mol, $M_H = 1.0$ g/mol, and $\alpha$ is the ratio of moles of hydrogen to moles of carbon in the fuel. The subscripts b and dil represent the background and post-dilution concentrations of a species. The derivation of this equation can be found in AIR6241 (2013). A similar form of the equation is used for number emissions.

To calculate the uncertainty in the MV, we must combine the uncertainties of each EI measurement. For this task, we assume that $\dot{m}_{f,i}$ and $F_{00}$ have negligible uncertainty. The uncertainty in each value required for estimating the EI is defined by the SAE E31 team, and the key values are included in Table 1.

**Table 1.** Uncertainty of each component of the nvPM mass and number measurement system (reproduced from CAEP/12-WG3-ECTG/6-WP/08)

| | **Mass** | **Number** |
|---|---|---|
| Instrument $\left(\frac{u(\mathrm{nvPM}_m)}{\mathrm{nvPM}_m}\right)$ | $30\ \mu\mathrm{g/m^3}$ + 13% | $6\times10^4/\mathrm{cm}^3$ + 7% |
| Dilution factor 1 $\left(\frac{u(\mathrm{DF}_1)}{\mathrm{DF}_1}\right)$ | 4% | 4% |
| $CO_2$ concentrations $\left(\frac{u([\mathrm{CO_2}]_{\mathrm{dil}})}{[\mathrm{CO_2}]_{\mathrm{dil}}}, \left(\frac{u([\mathrm{CO_2}]_{\mathrm{b}})}{[\mathrm{CO_2}]_{\mathrm{b}}}\right)\right)$ | 4% | 4% |
| Dilution factor 2 $\left(\frac{u(\mathrm{DF}_2)}{\mathrm{DF}_2}\right)$ | | 10% |
| Thermophoretic losses $\left(\frac{u(k_t)}{k_t}\right)$ | 2% | 2% |
| Fuel correction $\left(\frac{u(k_f)}{k_f}\right)$ | 12% | 12% |
| Instrument drift | 2% | 5% |
| Year-to-year line loss variability | 2% | 5% |
| Year-to-year CPC response change | - | 5% |
| VPR penetration | - | 10% |

We assume that all uncertain components follow a Gaussian distribution and are statistically independent. This allows us to combine uncertainties in quadrature. To calculate the relative uncertainties of each emissions index, $u_{r,c}(\mathrm{EI})$, quadrature is performed as follows:

$$u_{r,c}(\mathrm{EI}) = \frac{1}{\mathrm{EI}}\sqrt{\begin{array}{c}\left(\frac{\partial \mathrm{EI}}{\partial \mathrm{nvPM}_m} u_r(\mathrm{nvPM})\right)^2 + \left(\frac{\partial \mathrm{EI}}{\partial k_t} u_r(k_t)\right)^2 + \left(\frac{\partial \mathrm{EI}}{\partial k_f} u_r(k_f)\right)^2 + \\ \left(\frac{\partial \mathrm{EI}}{\partial [\mathrm{CO_2}]_{\mathrm{dil}}} u_r([\mathrm{CO_2}]_{\mathrm{dil}})\right)^2 + \left(\frac{\partial \mathrm{EI}}{\partial \mathrm{DF}_1} u_r(\mathrm{DF}_1)\right)^2 + \left(\frac{\partial \mathrm{EI}}{\partial [\mathrm{CO_2}]_{\mathrm{b}}} u_r([\mathrm{CO_2}]_{\mathrm{b}})\right)^2\end{array}}$$

where $u_r(X)$ is the relative uncertainty of component $X$ as defined in Table 1. Finally, to obtain the uncertainty in the MV, we again use quadrature, assuming that the uncertainty at each mode of operation is independent and follows a Gaussian distribution.

To identify potential options for the no-change criteria, we estimate the uncertainty of EIs and MVs for engines with reported data. Emissions are converted to concentrations by estimating the volumetric flow rate through the engine. The approach for this is described in detail in Agarwal et al. (2019). We can then propagate uncertainties using the previous set of equations. This process is conducted for all engines with reported data.

Figures 1 and 2 show the relative uncertainty in nvPM mass and particle number EI, respectively, for all engines in the ICAO Engine Emissions Databank (EDB). In both cases, the uncertainty increases as emissions decrease, because of the instrument limit of detection of 30 µg/m³ and $6 \times 10^4$ particles/cm³. Both figures are colored according to the mode of operation. The difference by mode is driven by the conversion from concentration to EI, thus leading to a dependence on thrust setting in the relationship between EI and relative uncertainty.

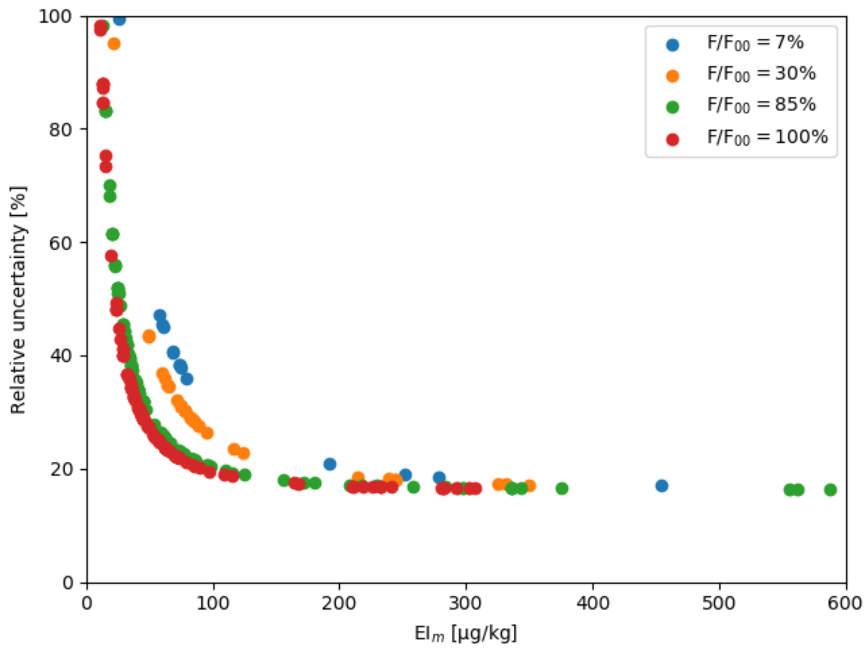


**Figure 1.** Relative uncertainty in mass emissions index as a function of mass emissions index.

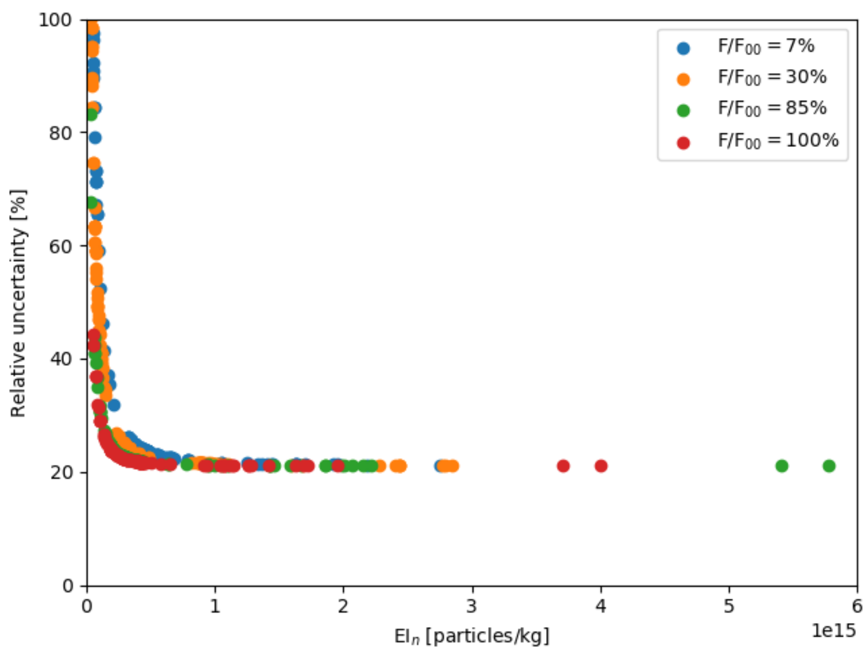


**Figure 2.** Relative uncertainty in number emissions index as a function of number emissions index.

Figures 3 and 4 show the relative uncertainty in nvPM mass and number MV ($D_{\mathrm{p}}/F_{\mathrm{oo}}$). As with the emissions index, the uncertainty in the metric value increases as the metric value decreases. This relationship can be modeled using an inverse proportional function, as shown in each figure. The relationship shows substantial scatter caused by the differing contributions of each mode of operation to the overall $D_p$value. The relationships show that the uncertainty tends toward 12.5% for mass and 9.9% for number.

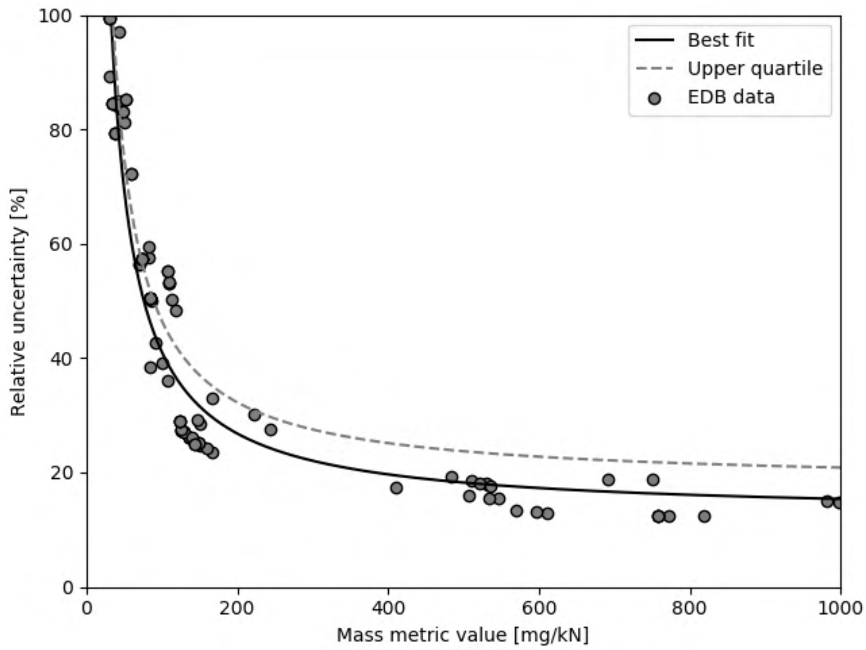


**Figure 3.** Relative uncertainty in mass metric value as a function of the mass metric value, with best fit curve and upper quartile.

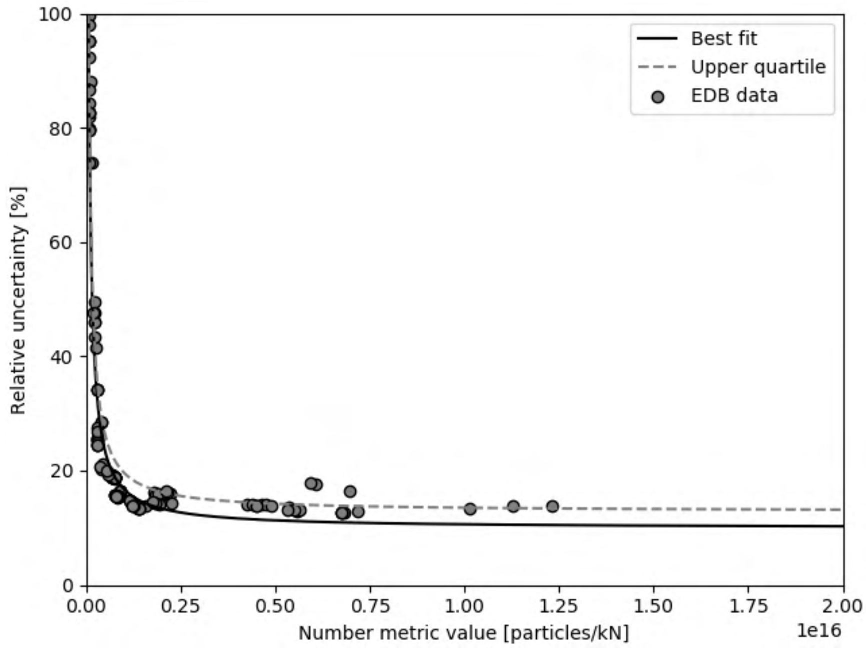


**Figure 4.** Relative uncertainty in the number metric value as a function of the number metric value, with best fit curve and upper quartile.

We define the no-change criteria as a piecewise continuous function. Below a threshold metric value, we use the absolute uncertainty to determine the no-change criteria. Above this threshold, we use the relative uncertainty. To define the values of the absolute and relative uncertainties in each region, we use two approaches. The first approach starts with the upper quartile of the best-fit relationships found in Figures 3 and 4. We select the threshold metric value and identify the relative uncertainty according to the upper quartile of the best-fit relationships. This also defines the absolute uncertainty, which is calculated by multiplying the relative uncertainty with the metric value. This is used to determine the no-change criteria below the threshold metric value. The second approach is to freely define both the threshold metric value and the relative uncertainty. The absolute uncertainty is defined the same way as in the first approach.

Six sample no-change criteria for mass emissions are shown in Figure 5, and four sample no-change criteria for number emissions are shown in Figure 6. Two options (blue and orange lines) use the upper quartiles of the best-fit relationship. The green lines show a rounded version of the blue no-change criteria. Finally, additional options are provided in red for mass and number, and purple and brown for only mass, wherein the threshold value and relative uncertainty are set separately. These can maintain a similar absolute uncertainty to the blue and green lines but have lower relative uncertainty for emissions above their respective thresholds. A range of options is provided to showcase this balancing effect.

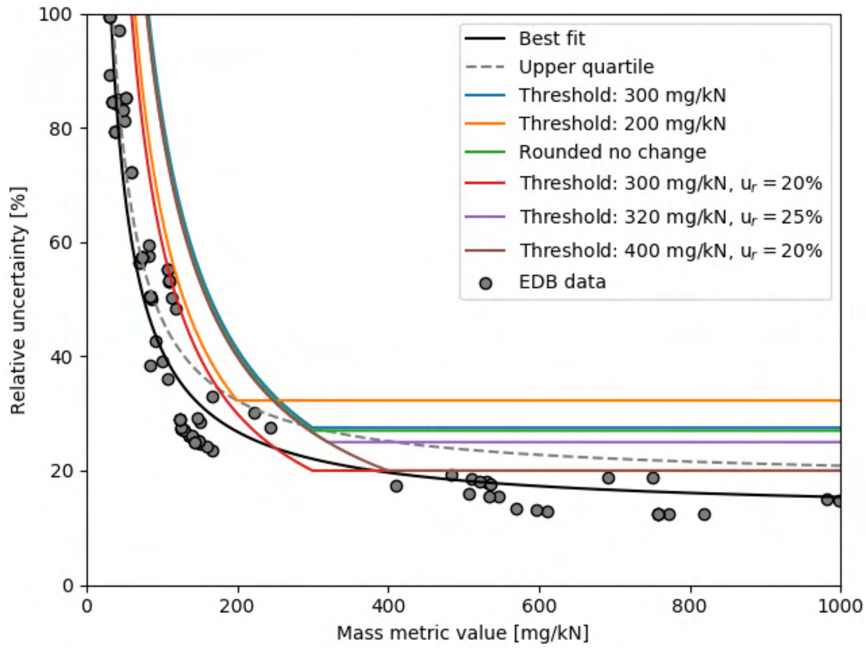


**Figure 3.** As in Figure 3, but including six options for the mass no-change criterion.

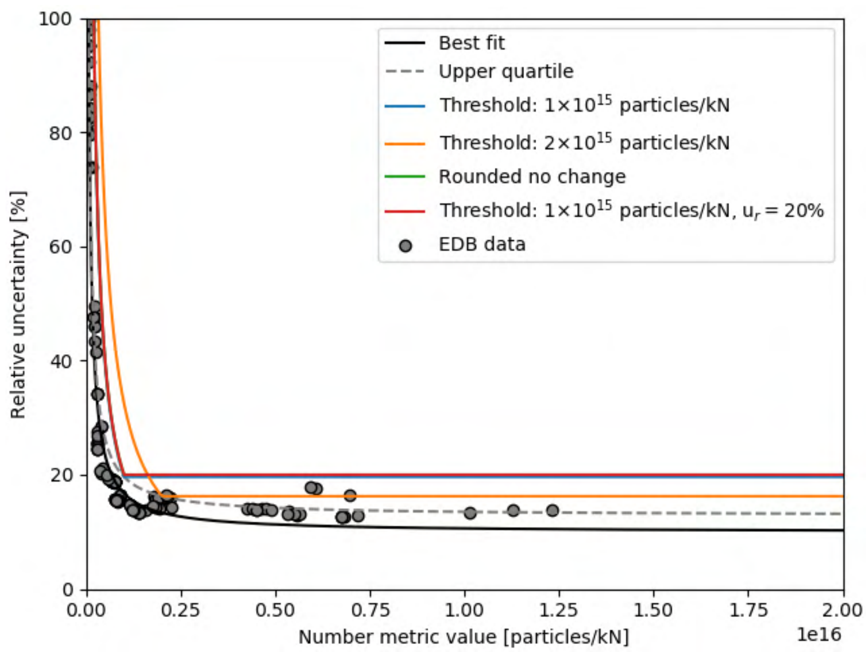


**Figure 4.** As in Figure 4, but including four options for the number no-change criterion.

The potential no-change criteria indicate a balance between increasing the uncertainty for low emissions and the constant uncertainty at higher emissions. The blue, green, and purple options are considered to balance both of these levels, providing sufficient spacing above the best-fit line and the scatter of the uncertainty values calculated from the EDB.

## Milestone
The complete analysis was presented to the FAA and in a working paper for CAEP/12-WG3-ECTG/6.

## Major Accomplishments
This work was presented to CAEP/12-WG3-ECTG/6 and used to help the group reach consensus on a no-emissions-change criterion for nvPM mass and number emissions.

## Publications
None

## Outreach Efforts
Our results have been communicated to the FAA and CAEP-WG3 in a detailed report and presentation.

## Awards
None

## Student Involvement
Graduate student Akshat Agarwal conducted the analyses and presented the work.

## Plans for Next Period
This task is complete.

## References
E-31P Particulate Matter Committee. (2013). Procedure for the continuous sampling and measurement of non-volatile particle emissions from aircraft turbine engines (Report No. SAE AIR 6241). SAE International.

Agarwal, A., Speth, R. L., Fritz, T. M., Jacob, S. D., Rindlisbacher, T., Iovinelli, R., Owen, B., Miake-Lye, R. C., Sabnis, J. S., & Barrett, S. R. H. (2019). SCOPE11 method for estimating aircraft black carbon mass and particle number emissions. Environmental Science and Technology, *53*(3), 1364–1373. https://doi.org/10.1021/acs.est.8b04060

# Task 2 - Extending the nvPM Fuel Correction Method for Blended Fuels
Massachusetts Institute of Technology

## Objective
This task aimed to identify the accuracy for the nvPM fuel correction method for blended fuels and compare it to other formulations.

## Research Approach
Current fuel standards allow aircraft engines to use conventional fuels that are blended with up to 50% by volume of biofuels. Biofuels tend to have higher hydrogen content than conventional jet fuels; therefore, blended fuels also have higher hydrogen content than conventional jet fuels. Increasing the hydrogen content of a fuel is expected to decrease nvPM emissions (Moore et al., 2017; Speth et al., 2015). To assess the reduction in emissions, the modeling and database group (MDG) requested WG3 to provide an approach to estimate the decrease in emissions associated with using blended fuels. In this task, we first assessed the accuracy of using the current certification fuel correction approach developed during CAEP/11. In addition, we developed a different formulation that assumes a quadratic relationship between the change in emissions and hydrogen content.

To test the performance and fit coefficients of all model, we combine several engine measurement datasets that comprise six different engines for mass emissions and two additional engines for number emission (Bulzan et al. 2010; Beyersdorf et al. 2014; Timko et al. 2011; 2010; Corporan et al. 2013; 2011; Cain et al. 2013; Corporan et al. 2010; Brem et al. 2015). In addition, we included auxiliary-power-unit (APU) emissions data provided by Prem Lobo (personal communication). Two forms of fits were tested on these datasets. The first follows an exponential trend in hydrogen content (*H*) and thrust setting ($F/F_{00}$) as:

$$\hat{E} = \exp\big((k_1 + k_2 F/F_{00})(H_0 - H)\big)$$

where $\hat{E}$ is the relative change in emissions, $H_0 = 13.8\%$ is the reference-fuel hydrogen content, and $k_1$ and $k_2$ are coefficients to be fitted. The second form assumes a quadratic relationship in the hydrogen content as:

$$\hat{E} = (1 - \tilde{H})\big[(k_1 + k_2\hat{F})\tilde{H} + 1\big]$$

where $\tilde{H} = \frac{H - H_0}{H_\infty - H_0}$, and $H_\infty$, $k_1$, and $k_2$ are coefficients to be fitted. Both forms are fitted to the entire dataset, and the coefficients are shown in Table 2 below. This table also includes the coefficients used for the certification fuel correction approach.

**Table 2.** Fitted coefficient values for all models tested

| | Certification | | Exponential refitted | | Quadratic | |
|---|---|---|---|---|---|---|
| | Mass | Number | Mass | Number | Mass | Number |
| $k_1$ | 1.12 | 1.05 | 1.33 | 1.11 | −1.25 | −1.30 |
| $k_2$ | −0.95 | −0.99 | −0.79 | −0.69 | 1.54 | 1.98 |
| $H_\infty$ | | | | | 15.92 | 15.93 |

The performance of the certification, exponential refitted, and quadratic approaches is shown in Figures 7-9. The certification approach (Figure 7) exhibits low error for relative mass and number emissions above 1.0. This result is expected because the model was fitted to this set of CFM56-7 data. Below this range, the performance degrades, and the approach tends to find a bias of −0.10 for mass and −0.09 for number. After refitting the coefficients in the certification approach for all available data (Figure 8), the overall performance improves, with the mean absolute error reducing by 20% for mass and 12.5% for number, and the mean error reducing by a factor of 3.2 and 6.0 for mass and number, respectively. The main region where the approach improves for biofuel prediction is for relative emissions below 1.0, which shows lower variance away from the parity line. Above relative emissions of 1.0, the approach does not perform as well as the certification approach, and high bias is present in the results. Finally, the results of the quadratic approach (Figure 9) show the lowest bias, by a factor of 1.9 for mass and factor of 12.5 for number, as compared with the refitted exponential approach. This approach balances the performance at all relative emissions levels (above and below 1.0) better than the exponential form.

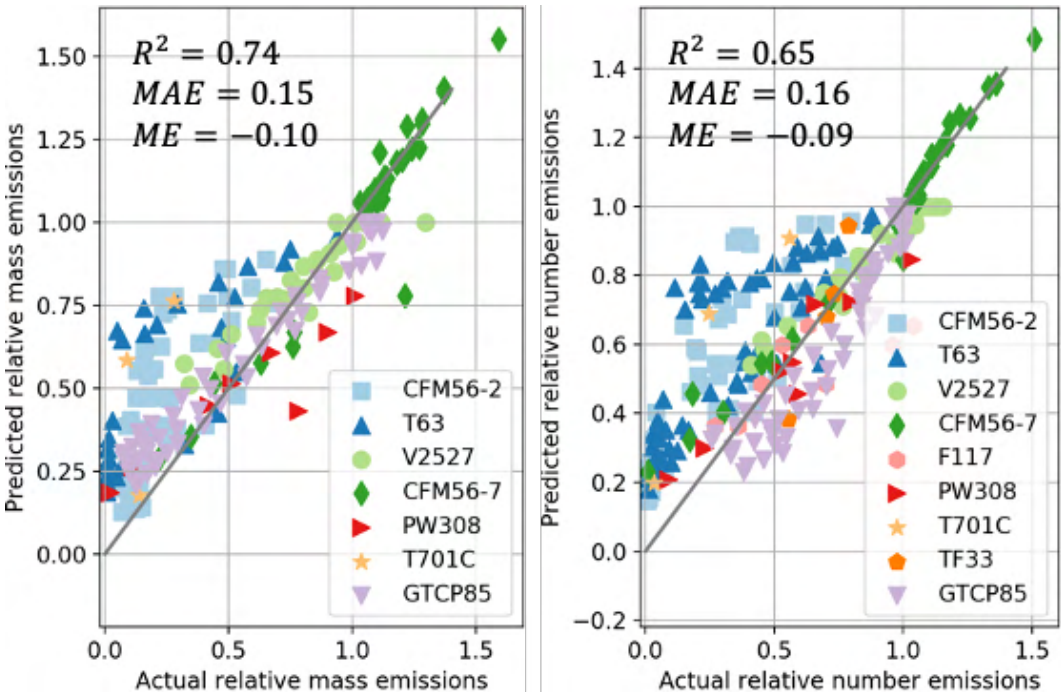


**Figure 5.** Actual/measured versus predicted relative mass emissions (left) and number emissions (right) using the certification fuel approach.

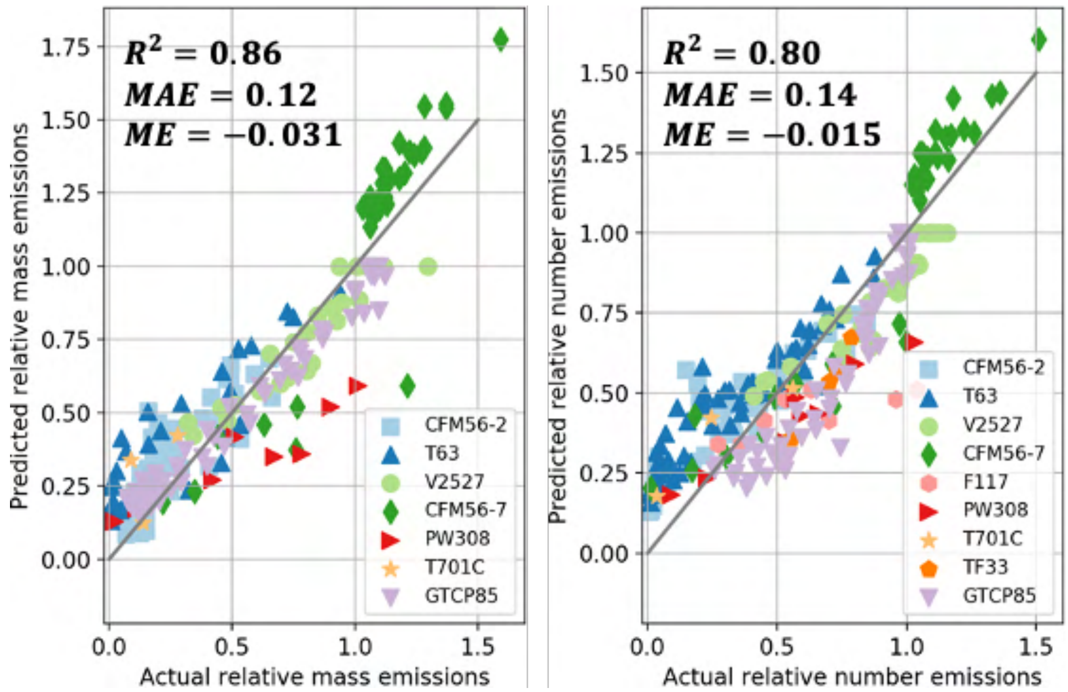


**Figure 6.** Actual/measured versus predicted relative mass emissions (left) and number emissions (right) using the exponential refitted approach.

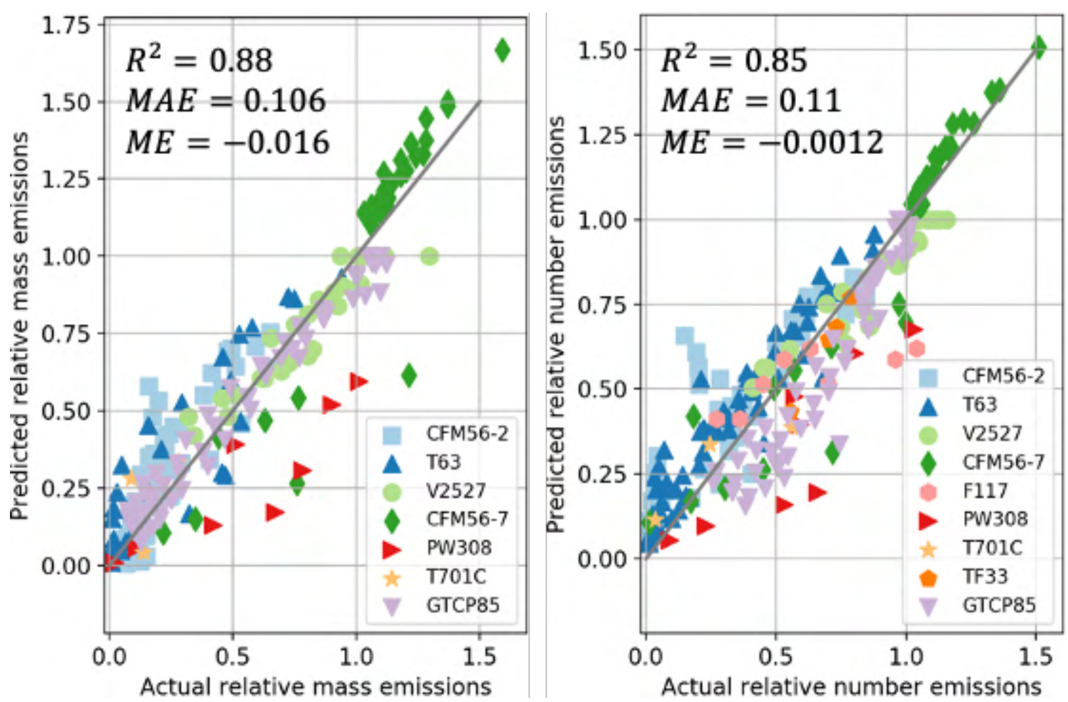


**Figure 7.** Actual/measured versus predicted relative mass emissions (left) and number emissions (right) using the quadratic approach.

To further understand the differences between these methods arising from the different fuel sources and measurement systems used in the different data sets, the error metrics ($R^2$, MAE, and ME) were evaluated for each of these different subsets, as shown in Figures 10–12 respectively.

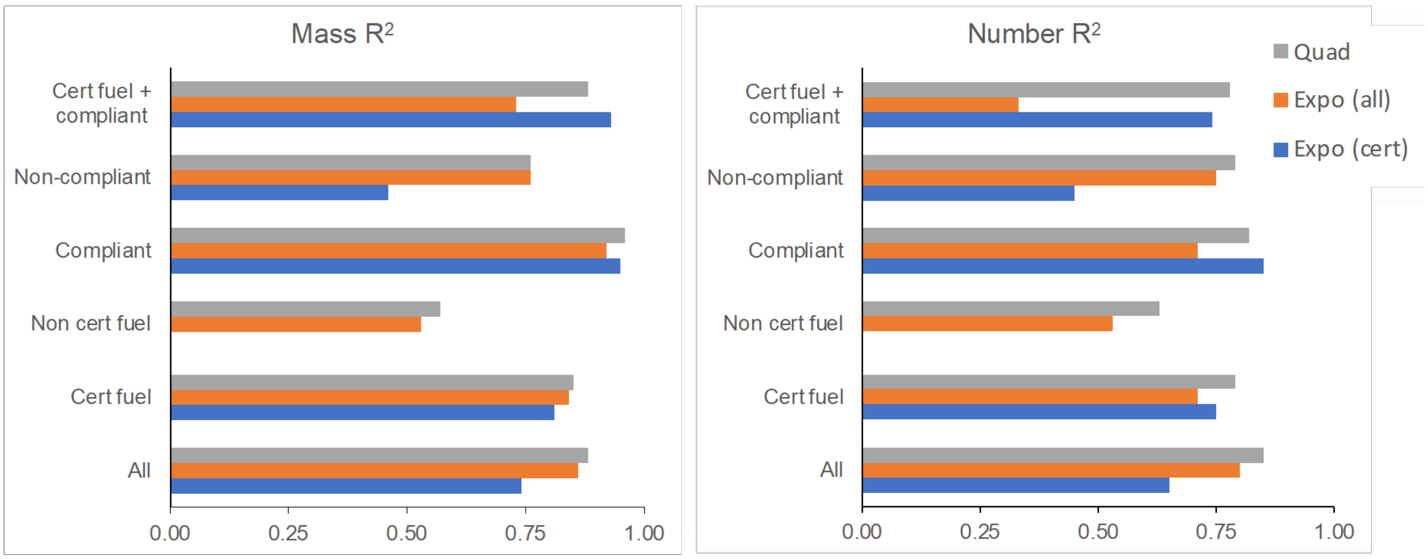


**Figure 10.** $R^2$ of each fuel correction formula for mass and number emissions, evaluated for different data subsets.

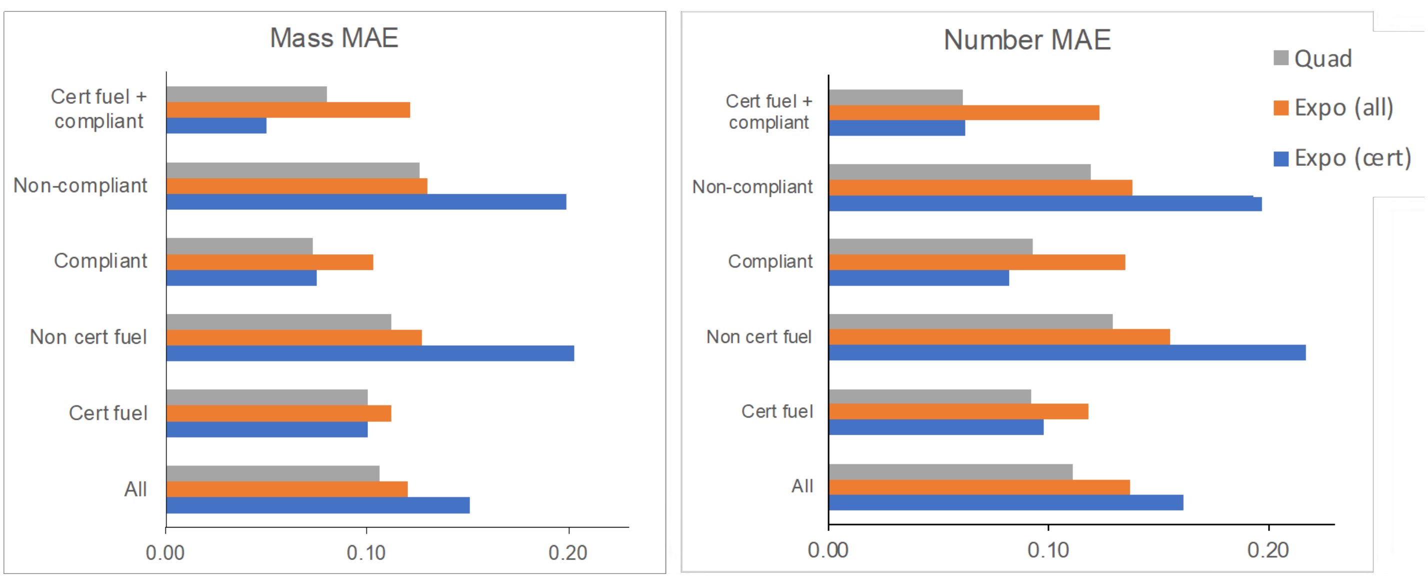


**Figure 11.** Mean absolute error of each fuel correction formula for mass and number emissions, evaluated for different data subsets.

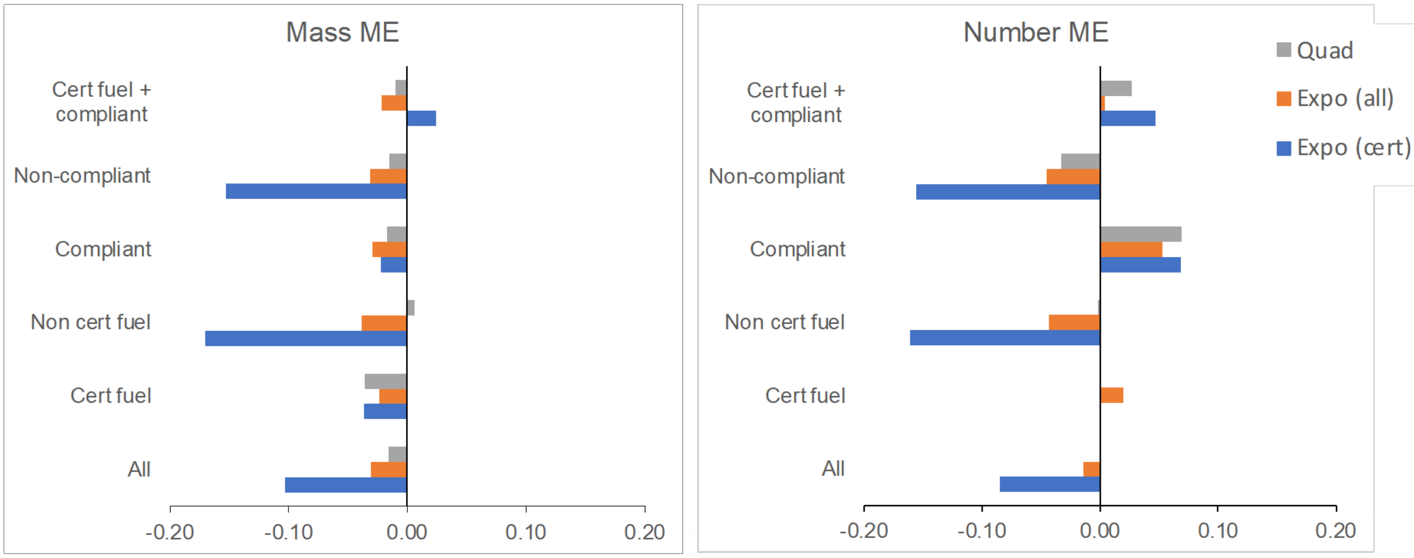


**Figure 12.** Mean error of each fuel correction formula for mass and number emissions, evaluated for different data subsets.

For the $R^2$ metric (Figure 10), in which values closer to 1 indicate better performance, the certification method performs best. This finding is expected because this data set was used to develop this correction. In all other cases, the quadratic approach tends to perform best, but the extent to which it outperforms the other methods varies with different data subsets. With this metric, very little difference is found between the quadratic approach and the refitted exponential relationship.

For the mean absolute error (Figure 11), the certification method again performs the best on the smaller data set that was used to fit its parameters. For all other combinations of datasets, the quadratic approach yields the best results. The effect of refitting the exponential relationship has varying effects depending on the target dataset.

Finally, the mean error (Figure 12) shows that the quadratic approach has the lowest bias, except when only measurements taken with certification-compliant fuels and measurement systems are considered, in which case the two methods perform similarly. However, for other data subsets, the bias of the quadratic approach is much smaller than the bias of the exponential approach.

## Milestone
The results of this analysis were presented to FAA project managers and to members of the ECTG group under WG3 at the 7$^{th}$ meeting of CAEP/12-WG3.

## Major Accomplishments
None

## Publications
None

## Outreach Efforts
Our results have been communicated to the FAA and ICAO-CAEP in a detailed report and presentation.

## Awards
None

## Student Involvement
Graduate student Akshat Agarwal conducted the analysis.

## Plans for Next Period
This task is complete.

## References

Beyersdorf, A. J., M. T. Timko, L. D. Ziemba, D. Bulzan, E. Corporan, S. C. Herndon, R. Howard, et al. 2014. "Reductions in Aircraft Particulate Emissions Due to the Use of Fischer–Tropsch Fuels." *Atmospheric Chemistry and Physics* 14 (1): 11–23. https://doi.org/10.5194/acp-14-11-2014.

Brem, Benjamin T., Lukas Durdina, Frithjof Siegerist, Peter Beyerle, Kevin Bruderer, Theo Rindlisbacher, Sara Rocci-Denis, et al. 2015. "Effects of Fuel Aromatic Content on Nonvolatile Particulate Emissions of an In-Production Aircraft Gas Turbine." *Environmental Science and Technology*, October. https://doi.org/10.1021/acs.est.5b04167.

Bulzan, Dan, Bruce Anderson, Changlie Wey, Robert Howard, Edward Winstead, Andreas Beyersdorf, Edwin Corporan, et al. 2010. "Gaseous and Particulate Emissions Results of the NASA Alternative Aviation Fuel Experiment (AAFEX)," October, 1195–1207. https://doi.org/10.1115/GT2010-23524.

Cain, Jeremy, Matthew J. DeWitt, David Blunck, Edwin Corporan, Richard Striebich, David Anneken, Christopher Klingshirn, W. M. Roquemore, and Randy Vander Wal. 2013. "Characterization of Gaseous and Particulate Emissions From a Turboshaft Engine Burning Conventional, Alternative, and Surrogate Fuels." *Energy & Fuels* 27 (4): 2290–2302. https://doi.org/10.1021/ef400009c.

Corporan, Edwin, Matthew J. DeWitt, Christopher D. Klingshirn, David Anneken, Linda Shafer, and Richard Streibich. 2013. "Comparisons of Emissions Characteristics of Several Turbine Engines Burning Fischer-Tropsch and Hydroprocessed Esters and Fatty Acids Alternative Jet Fuels." In , 425–36. American Society of Mechanical Engineers Digital Collection. https://doi.org/10.1115/GT2012-68656.

Corporan, Edwin, Matthew J. DeWitt, Christopher D. Klingshirn, Richard Striebich, and Meng-Dawn Cheng. 2010. "Emissions Characteristics of Military Helicopter Engines with JP-8 and Fischer-Tropsch Fuels." *Journal of Propulsion and Power* 26 (2): 317–24. https://doi.org/10.2514/1.43928.

Corporan, Edwin, Tim Edwards, Linda Shafer, Matthew J. DeWitt, Christopher Klingshirn, Steven Zabarnick, Zachary West, Richard Striebich, John Graham, and Jim Klein. 2011. "Chemical, Thermal Stability, Seal Swell, and Emissions Studies of Alternative Jet Fuels." *Energy & Fuels* 25 (3): 955–66. https://doi.org/10.1021/ef101520v.

Moore, Richard H., Kenneth L. Thornhill, Bernadett Weinzierl, Daniel Sauer, Eugenio D'Ascoli, Jin Kim, Michael Lichtenstern, et al. 2017. "Biofuel Blending Reduces Particle Emissions from Aircraft Engines at Cruise Conditions." *Nature* 543 (7645): 411–15. https://doi.org/10.1038/nature21420.

Speth, Raymond L., Carolina Rojo, Robert Malina, and Steven R. H. Barrett. 2015. "Black Carbon Emissions Reductions from Combustion of Alternative Jet Fuels." *Atmospheric Environment* 105 (Supplement C): 37–42. https://doi.org/10.1016/j.atmosenv.2015.01.040.

Timko, M. T., Scott C. Herndon, Elena de la Rosa Blanco, Ezra C. Wood, Zhenhong Yu, Richard C. Miake-Lye, W. Berk Knighton, Linda Shafer, Matthew J. DeWitt, and Edwin Corporan. 2011. "Combustion Products of Petroleum Jet Fuel, a Fischer–Tropsch Synthetic Fuel, and a Biomass Fatty Acid Methyl Ester Fuel for a Gas Turbine Engine." *Combustion Science and Technology* 183 (10): 1039–68. https://doi.org/10.1080/00102202.2011.581717.

Timko, M. T., Z. Yu, T. B. Onasch, H.-W. Wong, R. C. Miake-Lye, A. J. Beyersdorf, B. E. Anderson, et al. 2010. "Particulate Emissions of Gas Turbine Engine Combustion of a Fischer—Tropsch Synthetic Fuel." *Energy & Fuels* 24 (11): 5883–96. https://doi.org/10.1021/ef100727t.

# Task 3 - Analyze Emissions Data Collected for the CAEP/10 nvPM Standard

Massachusetts Institute of Technology

## Objective

The objective of this task was to conduct an analysis of emissions data provided by engine manufacturers to satisfy the requirements of the CAEP/10 nvPM standard.

## Research Approach

The CAEP/10 nvPM standard includes reporting requirements for nvPM mass and number emissions measurements at the thrust settings used in the ICAO LTO cycle. For this task, we used this information to evaluate each engine and compare the results with the CAEP/11 nvPM mass and number standards for in-production and new type engines. This analysis provides information needed to understand possible industry responses to the CAEP/11 standards.

Figure 13 shows the nvPM and $NO_x$ emissions as a percentage of the new-type nvPM and $NO_x$ standards, for in-production engines for which nvPM emissions data were added to the ICAO Emissions Databank (EDB). Although all of these engines meet the applicable certification standards according to their date of type certification, some of these engines would not pass the CAEP/8 $NO_x$ standard if they were certified today, and some would not pass the CAEP/11 nvPM standard if they were certified after that standard becomes applicable on January 1, 2023. Specifically, five engines in three families would not pass the nvPM mass standard, whereas six other engine families include engines within 10% of the nvPM mass limit. Four in-production engines in two families would not pass the nvPM number standard, whereas two other engine families include engines within 10% of the limit.

The distribution of margins to the relevant limits differs among engine families. Whereas the margins to the CAEP/8 $NO_x$ limit vary between 10% and 55% (that is, no engine is below 45% of the CAEP/8 limit), the margins to the CAEP/11 nvPM standard are effectively as high 100% for some engines.

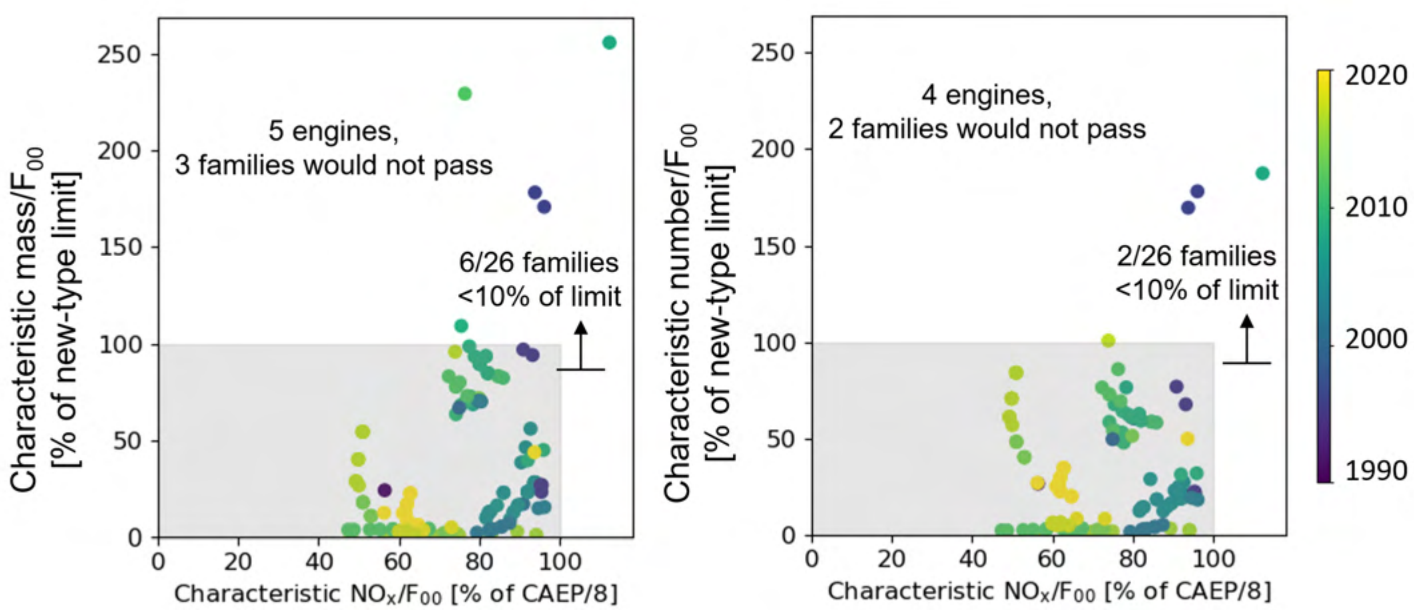


**Figure 13.** Performance of in-production engines relative to the CAEP/11 new-type limits for nvPM mass (left) and number (right) emissions (vertical axis) and to the CAEP/8 $NO_x$ regulation (horizontal axis).

Emissions data reported for an engine that has been recertified after a change to the combustor can provide insight into potential interdependencies between $NO_x$ and nvPM emissions. Figure 14 shows data for one such example using data from the EDB. Although the reasons for recertification are not reported in the EDB, the emissions results for this combustor show that $NO_x$ emissions increased by 5%–15% depending on the thrust condition, and nvPM mass emissions decreased by 20%–80%.

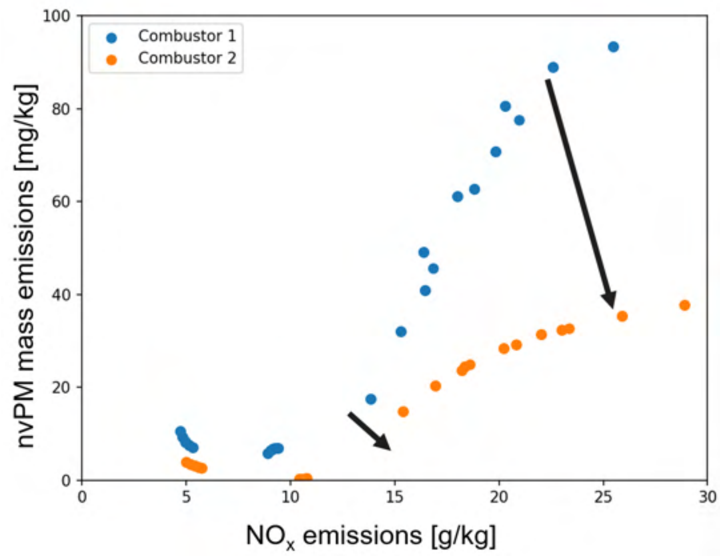


**Figure 14.** Changes in $NO_x$ and nvPM mass emissions after a combustor revision.

## Milestone
The complete analysis was presented to the FAA and the ECTG Emissions Data Analysis ad hoc group.

## Major Accomplishments
This work has been presented during CAEP/12-WG3-ECTG/7.

## Publications
None

## Outreach Efforts
Our results have been communicated to the FAA and CAEP/WG3 in a detailed report and presentation.

## Awards
None

## Student Involvement
Graduate student Akshat Agarwal conducted the analyses and presented the work.

## Plans for Next Period
This task is complete.

# Task 4 - Evaluating Cruise Emissions Based on Ground Measurements

Massachusetts Institute of Technology

## Objective

The objective of this task is to develop a modeling-based approach for estimating nvPM emissions at cruise and to use this approach to evaluate cruise emissions of different combustor technologies.

## Research Approach

Because of the lack of cruise emission data, cruise emission estimation methods such as $P_3T_3$ and fuel flow methods (Dubois & Paynter, 2006; Schaefer & Bartosch, 2013) are used to calculate the emissions profiles of aircraft operations. $P_3T_3$ and fuel flow methods were developed for conventional rich burn, quick-mix, lean burn (RQL)-style combustors (Samuelsen, 2006) and have not been rigorously evaluated for newer technologies such as lean, staged combustors (Foust et al, 2012). The LTO emission measurements available from certification tests do not cover the range of middle power percentage (30%–85%) in which the switching to lean combustion occurs for such combustors. Moreover, the prediction of nvPM emissions in these estimation methods is not included.

For this task, we will calibrate a reactor network model of a gas turbine combustor by using ground-based emissions measurements from the EDB. The primary zone of the combustor is split into several zero-dimensional reactors with different volumes and equivalent ratios. Such reactor network models have been successfully used to predict combustor emissions (Allaire, 2006; Moniruzzaman & Yu, 2012). Using an engine cycle deck developed in the Numerical Propulsion System Simulation (Claus et all, 1991) and matched to that engine's performance, we will calculate the combustor inlet conditions at cruise, and use the combustor model to evaluate the resulting nvPM mass and number emissions. We will apply this approach to an engine with an RQL combustor and to an engine with a lean, staged combustion system.

## Milestone

Validate the engine model by comparing it with EDB data and the conventional emission estimation methods.

## Major Accomplishments

None

## Publications

None

## Outreach Efforts

None

## Awards

None

## Student Involvement

None

## Plans for Next Period

After development of the model is completed, it will be validated against combustor rig test data which provides a surrogate for cruise-relevant conditions. The model will then be used to evaluate existing methods for predicting cruise emissions and to determine modifications that enhance the accuracy of those methods.

## References

Claus, R. W., Evans, A. L., Lylte, J. K., & Nichols, L. D. (1991). Numerical propulsion system simulation. Computing Systems in Engineering, *2*(4), 357-364.DuBois, D., & Paynter, G. C. (2006). Fuel Flow Method 2 for Estimating Aircraft Emissions. *SAE Transactions*, 1-14.

Schaefer, M., & Bartosch, S. (2013). Overview on fuel flow correlation methods for the calculation of NOx, CO and HC emissions and their implementation into aircraft performance software. *Institut für Antriebstechnik, Köln.*

Samuelsen, S. (2006). Rich burn, quick-mix, lean burn (RQL) combustor. *The Gas Turbine Handbook*, 227-233.
Foust, M., Thomsen, D., Stickles, R., Cooper, C., & Dodds, W. (2012). Development of the GE aviation low emissions TAPS combustor for next generation aircraft engines. In *50th AIAA aerospace sciences meeting including the new horizons forum and aerospace exposition* (p. 936).
Claus, R. W., Evans, A. L., Lylte, J. K., & Nichols, L. D. (1991). Numerical propulsion system simulation. *Computing Systems in Engineering*, *2*(4), 357-364.
Allaire, D. L. (2006). A physics-based emissions model for aircraft gas turbine combustors (Doctoral dissertation, Massachusetts Institute of Technology).
Moniruzzaman, C. G., & Yu, F. (2012). A 0D aircraft engine emission model with detailed chemistry and soot microphysics. Combustion and Flame, 159(4), 1670-1686.